

# Follow up on the incoherent $t, t'$

M. Hattawy

April 5, 2017

## 1 Overview

In our DVCS analysis, we considered the initial proton of the incoherent channel to be at rest, while this is not totally true because of the Fermi motion. Does this assumption is a good approximation? What other options can be used to minimize this effect on the calculated exclusive quantities?

Figure 1 presents the leading order handbag diagram of the incoherent DVCS channel off  $^4\text{He}$ . Ideally, the transferred momentum squared ( $t$ ) is defined using the initial and the final nucleons' 4-vectors as  $(p - p')^2$ . Then as a DVCS requirement,  $t$  has to be greater than a certain value ( $t_{min}$ ), which is defined using the kinematics of the incoming and the scattered electrons. Due to the knowledge lack of the initial proton's momentum, this cut maybe inaccurate, causes losing some good DVCS events and leading to inaccurate determination of the exclusivity cuts.

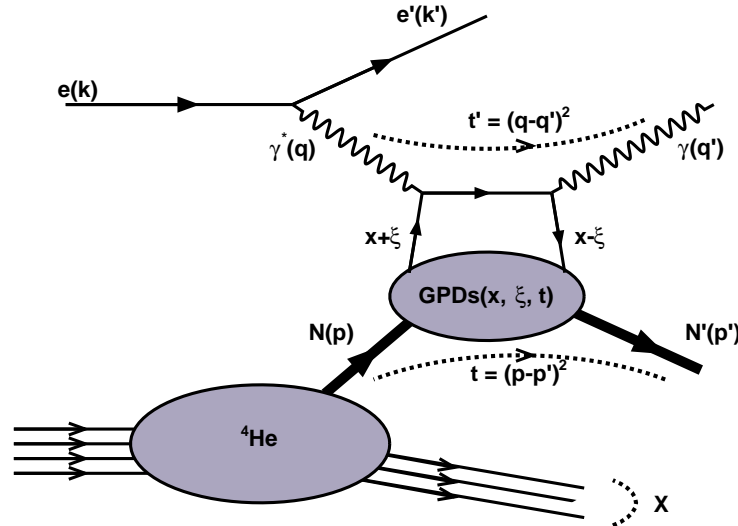


Figure 1: Representation of the leading order handbag diagram of the incoherent DVCS process off  $^4\text{He}$

## 2 Investigating the free proton DVCS data

Typically, the transferred momentum squared  $t$  is equal to the transferred momentum squared ( $t'$ ) defined between the virtual photon and the final-state real photon, as shown in Figure 1. While defining the momentum transferred as  $t'$  is a good way to pass the Fermi motion effect on the initial bound proton,  $t'$  suffers from the radiative effects. In this work, we study the radiative effects on  $t'$  using the CLAS available free proton DVCS data sets, E1-DVCS1 and E1-DVCS2.

Figure 2 presents the collected incoherent DVCS events from EG6 data binned into four bins in  $t$ . In order to evaluate the radiative effects on  $t'$  we carried out a full analysis on E1-DVCS1 and E1-DVCS2 data sets (free proton data). The collected free proton DVCS events in the two data sets were binned into similar bins as our incoherent DVCS events. The results are presented in figure 3. While the EG6 incoherent DVCS events show a relatively more smeared  $\frac{t'-t}{t}$  distributions than the free proton data sets, the free proton sets show a significant shifts specially at low  $t$  values.

## 3 $t'$ correction

One can see from the free proton DVCS sample, figure 3, that  $t'$  is slightly shifted compared to  $t$ , which is considered as the true value in the free proton case. This shift in  $t'$  is mainly induced by the radiative effects on the leptons. Before considering  $t'$  in the incoherent EG6 analysis,  $t'$  has to be corrected and the reconstructed free proton asymmetries have to be verified in order to estimate the associated systematic uncertainties. Figure 4 presents the distributions of  $t - t'$  as a function of  $t'$  for the free proton DVCS sample from E1-DVCS2 data before and after correcting  $t'$ . In figure 5, the distributions of figure 3 are shown after the  $t'$  corrections.

## 4 Comparing the $t$ and the corrected $t'$ asymmetries in the E1-DVCS2 data set

Here we compare the E1-DVCS2 free proton DVCS beam-spin asymmetries using  $t$  and the corrected  $t'$  to estimate the associated systematic uncertainties. Figure ?? presents the reconstructed  $A_{LU}$  as a function of  $\phi$  in the same binning as the incoherent EG6 DVCS channel. The binning in  $t$  and the corrected  $t'$  are the same. Figure 7 presents the  $A_{LU}$  at  $\phi = 90^\circ$  from the fits in figure 6, as a function of  $t$  and the corrected  $t'$  showing the estimated systematic uncertainties. No induced systematic uncertainties are observed on the  $Q^2$  and  $x_B$ , while some appear on  $t$ , which will be added to the EG6 incoherent asymmetries.

## 5 EG6 Incoherent DVCS channel

Here we apply the  $t'$  corrections that were extracted from the free proton asymmetries to the EG6 incoherent DVCS channel. Then, the asymmetries using  $t$  are compared to the ones reconstructed using the corrected  $t'$ . The results are presented in figures 8 and 9.

## 6 Conclusions

We improved the EG6 incoherent DVCS channel via the  $t'$  that is calculated using the virtual and the final state real photons with corrections based on similar analysis on the free proton DVCS sample using the same setup of CLAS detector. The  $Q^2$  and  $x_B$  dependences of the asymmetries

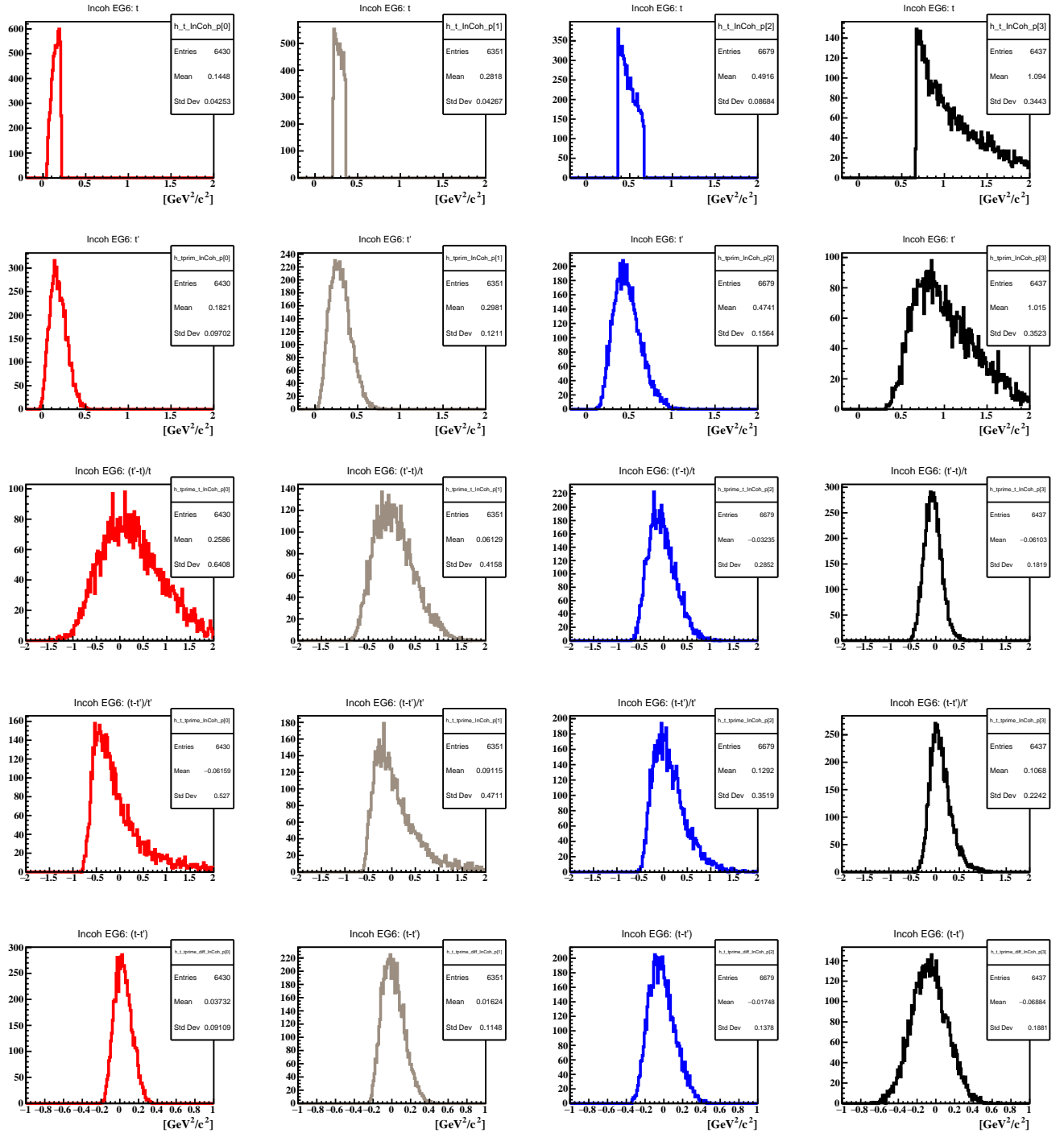


Figure 2: The EG6 incoherent DVCS sample. The first row presents the four bins in  $t$ . The second row shows the distribution of  $t'$  for the DVCS events in each bin in  $t$  in the first row plots. The third row shows  $\frac{t'-t}{t}$ . The 4<sup>th</sup> shows  $\frac{t-t'}{t'}$ , and the 5<sup>th</sup> shows  $t-t'$ .

have shown slight changes using  $t'$  rather than  $t$ , while the effect is bigger on the  $t$ -dependence, with overall changes are compatible with the statistical error bars. Based on the free proton DVCS data, no induced systematic uncertainties are observed on the  $Q^2$  and  $x_B$ , while some appear on  $t$ , which will be added to the EG6 incoherent asymmetries.

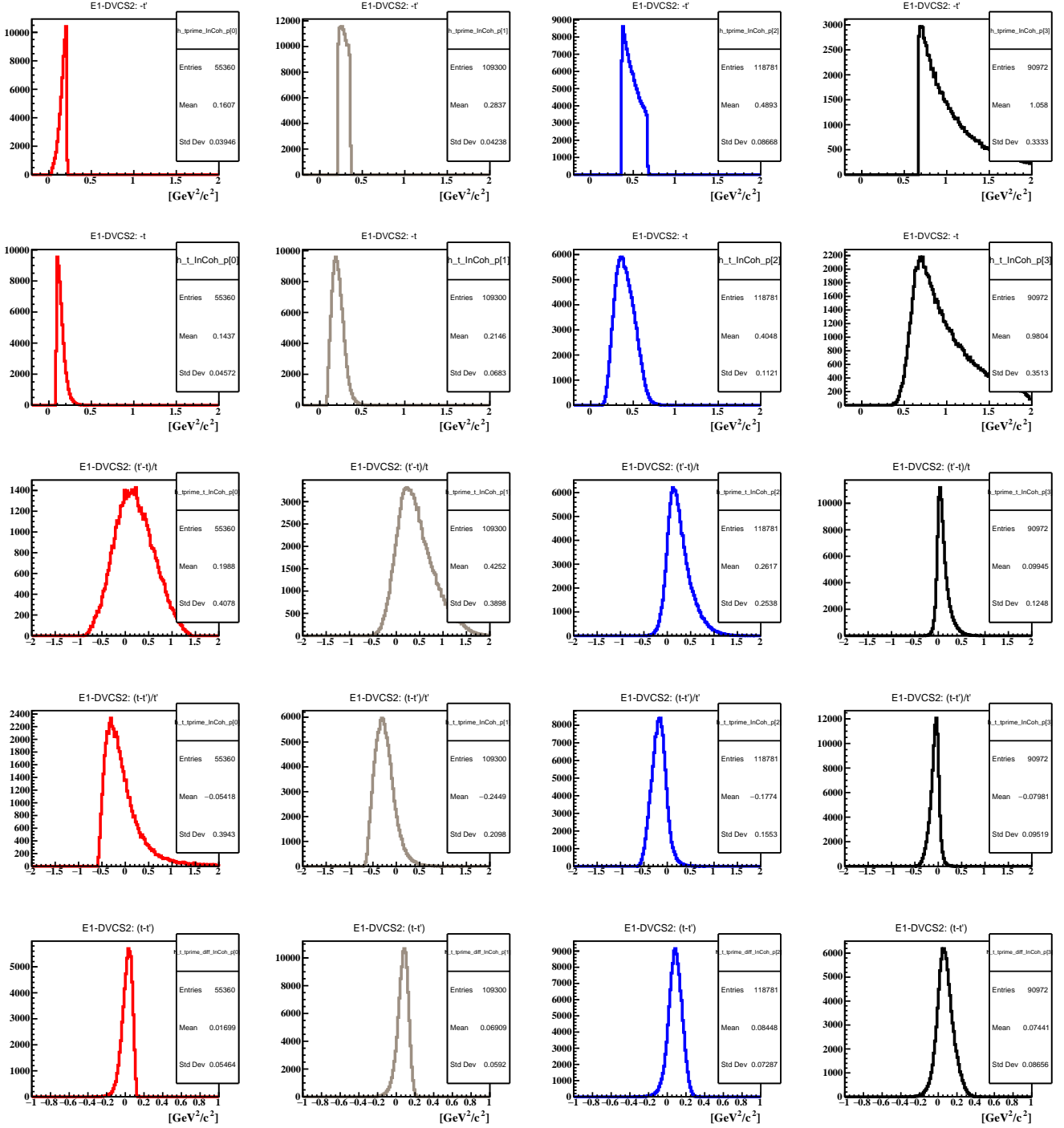


Figure 3: The E1-DVCS2 free proton DVCS sample BEFORE correcting  $t'$ . See the caption of figure 2 for plots description.

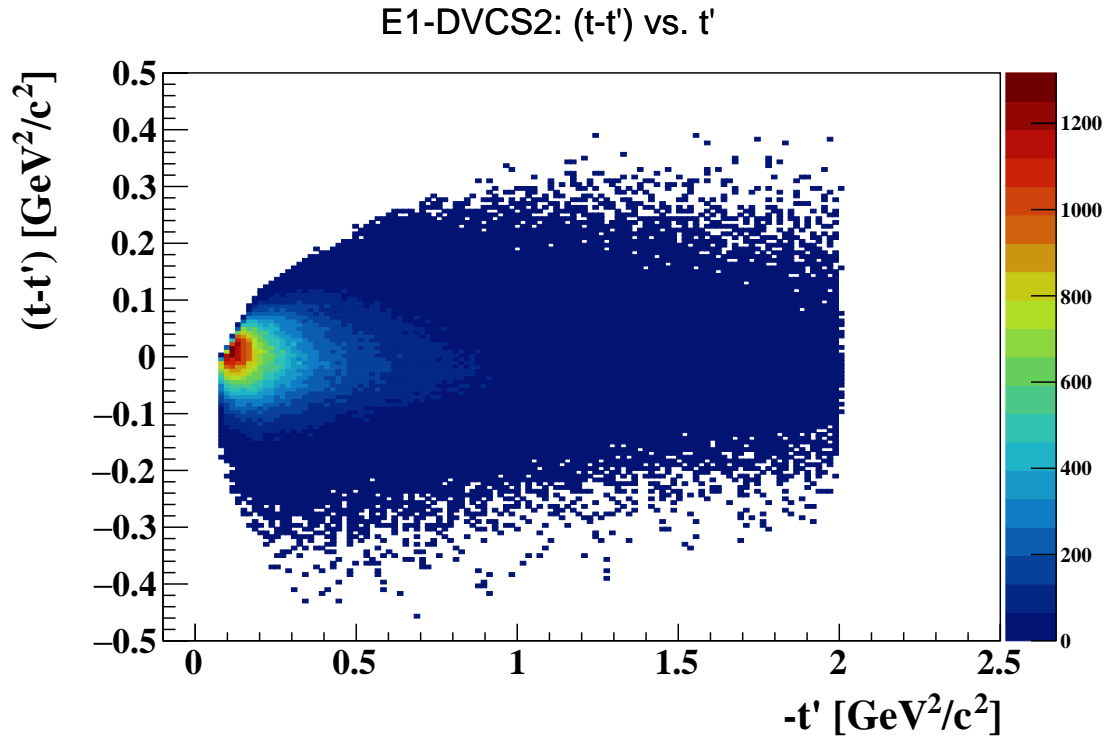
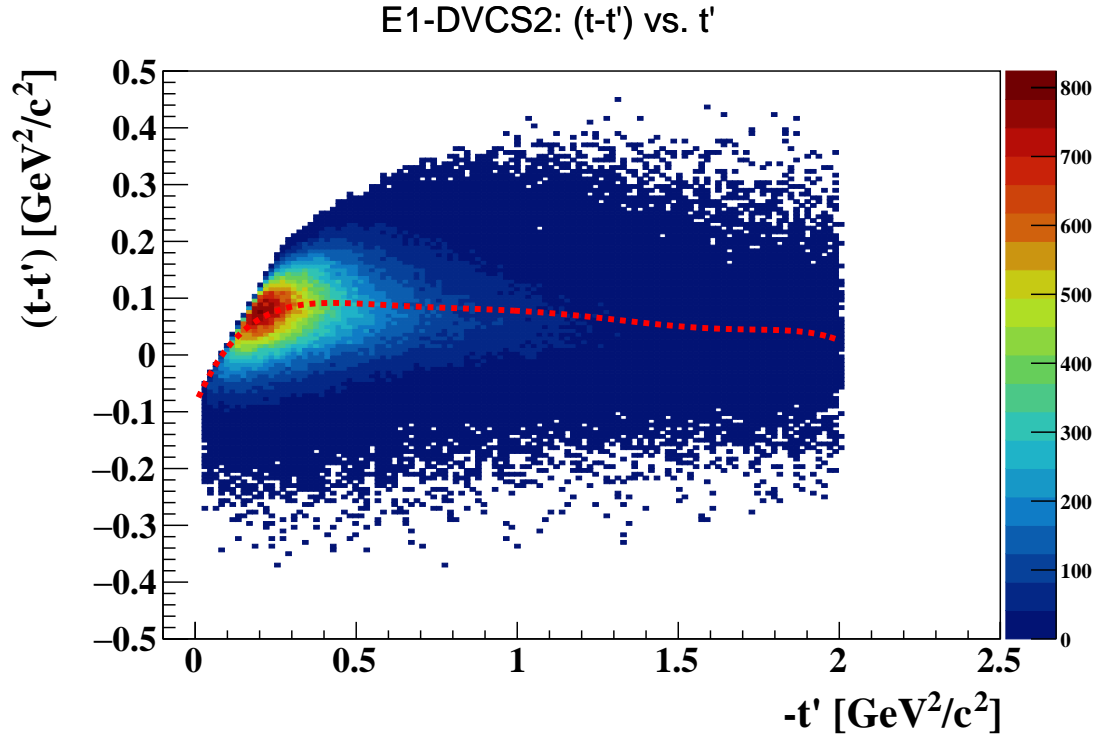


Figure 4: On top:  $t - t'$  as a function of  $t'$  for the E1-DVCS2 free proton DVCS sample BEFORE correcting  $t'$ . The red line is the extracted correction for  $t'$ . On bottom:  $t - t'$  as a function of  $t'$  after correcting  $t'$ .

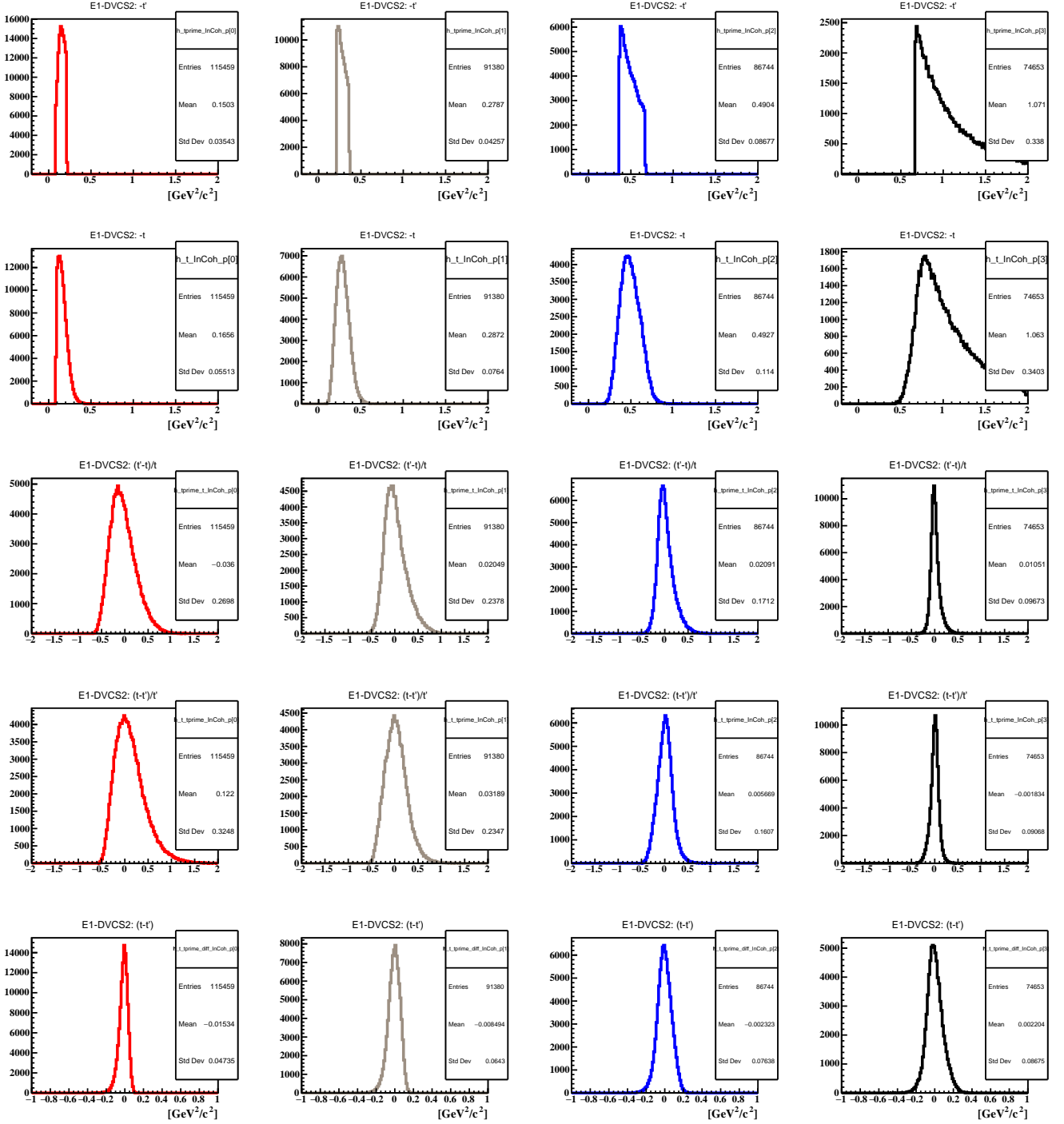


Figure 5: The E1-DVCS2 free proton DVCS sample AFTER correcting  $t'$ . See the caption of figure 2 for plots description.

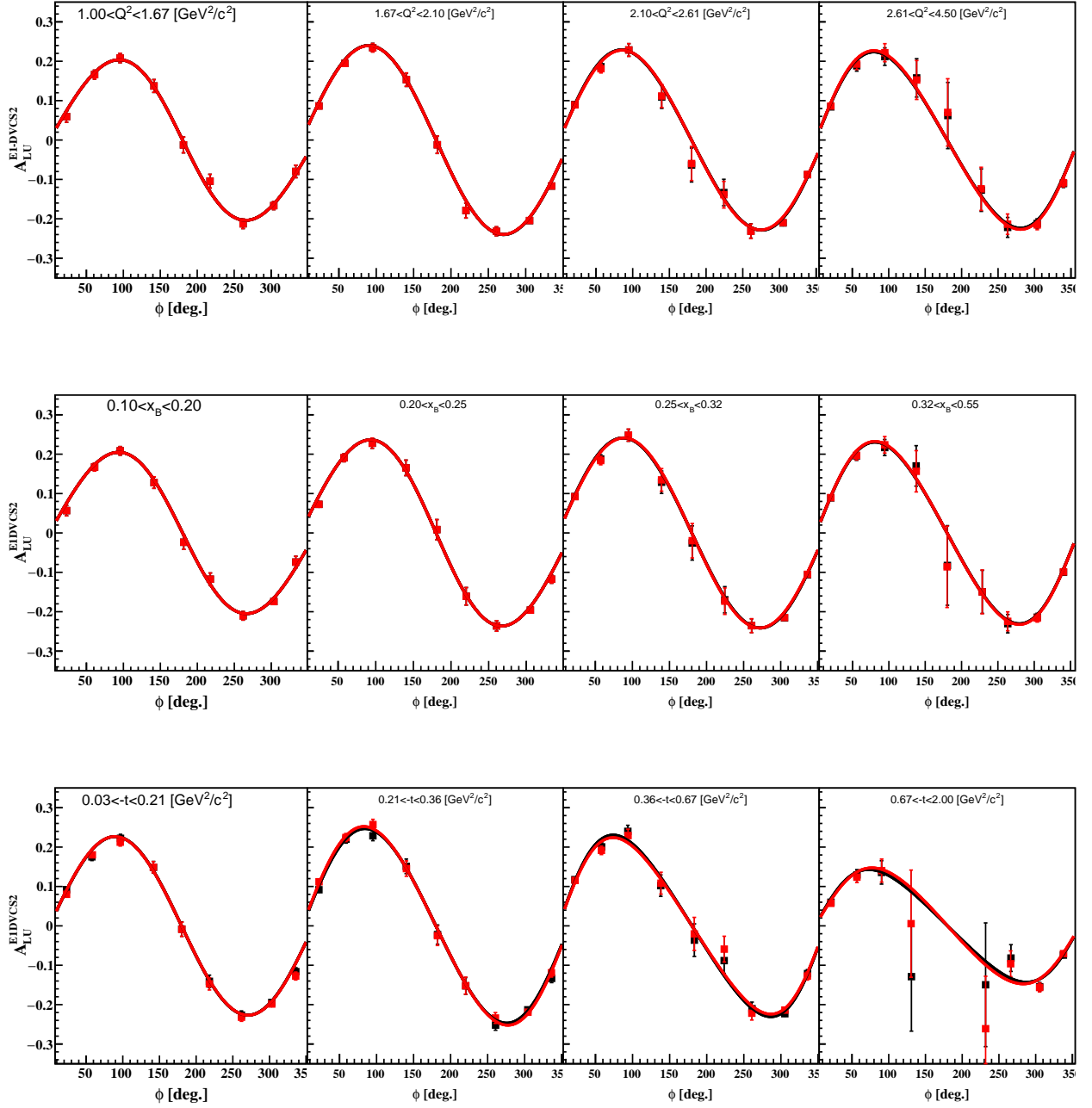


Figure 6: The reconstructed  $A_{LU}$  as a function of  $\phi$  for the collected E1-DVCS2 free proton DVCS sample using  $t$  in black points and using the corrected  $t'$  in red points. The lines represent fits in the form of  $\frac{\alpha \sin(\phi)}{1 + \beta \cos(\phi)}$  for the two sets of analysis.

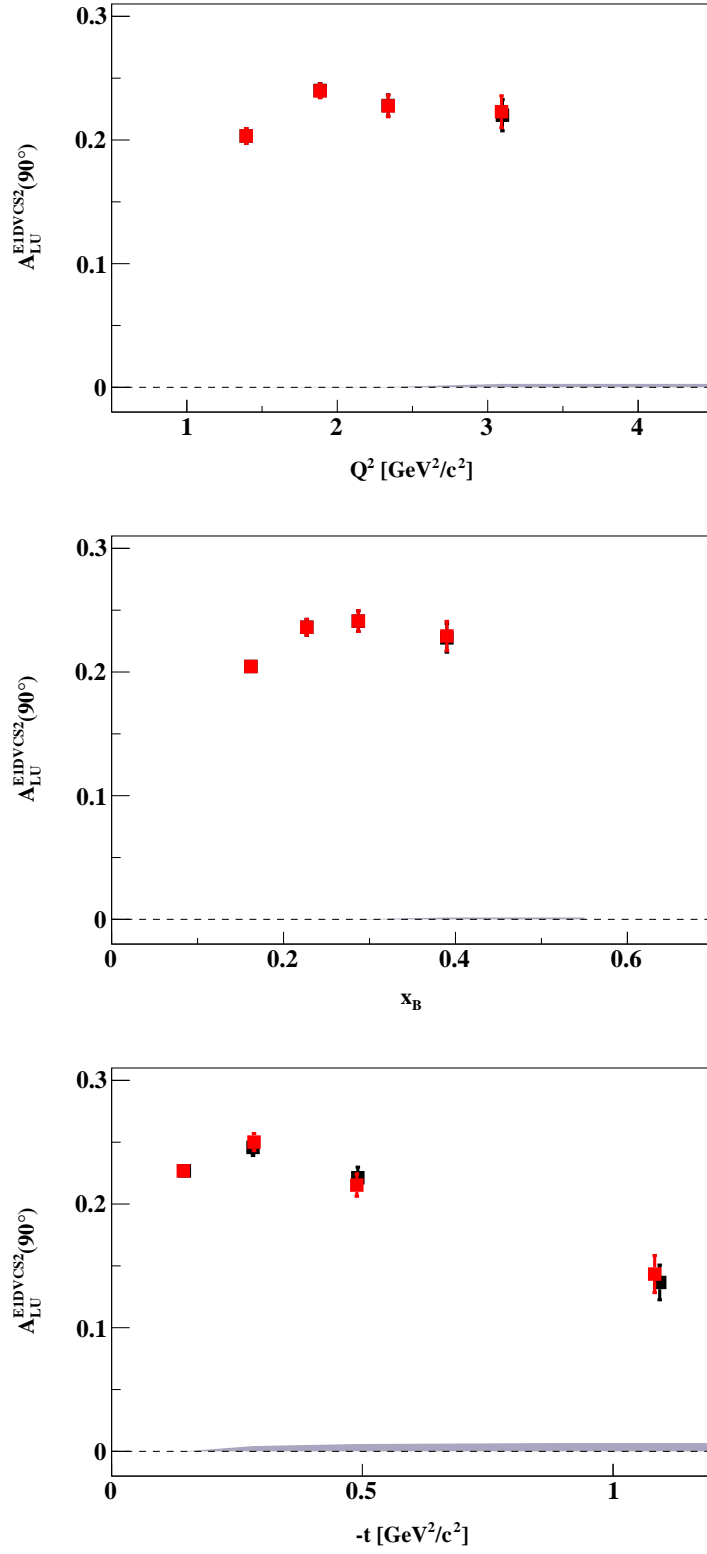


Figure 7:  $A_{LU}$  at  $\phi = 90^\circ$  from the fits in figure 6 as a function of  $t$  in black points and as a function of the corrected  $t'$  in red points.



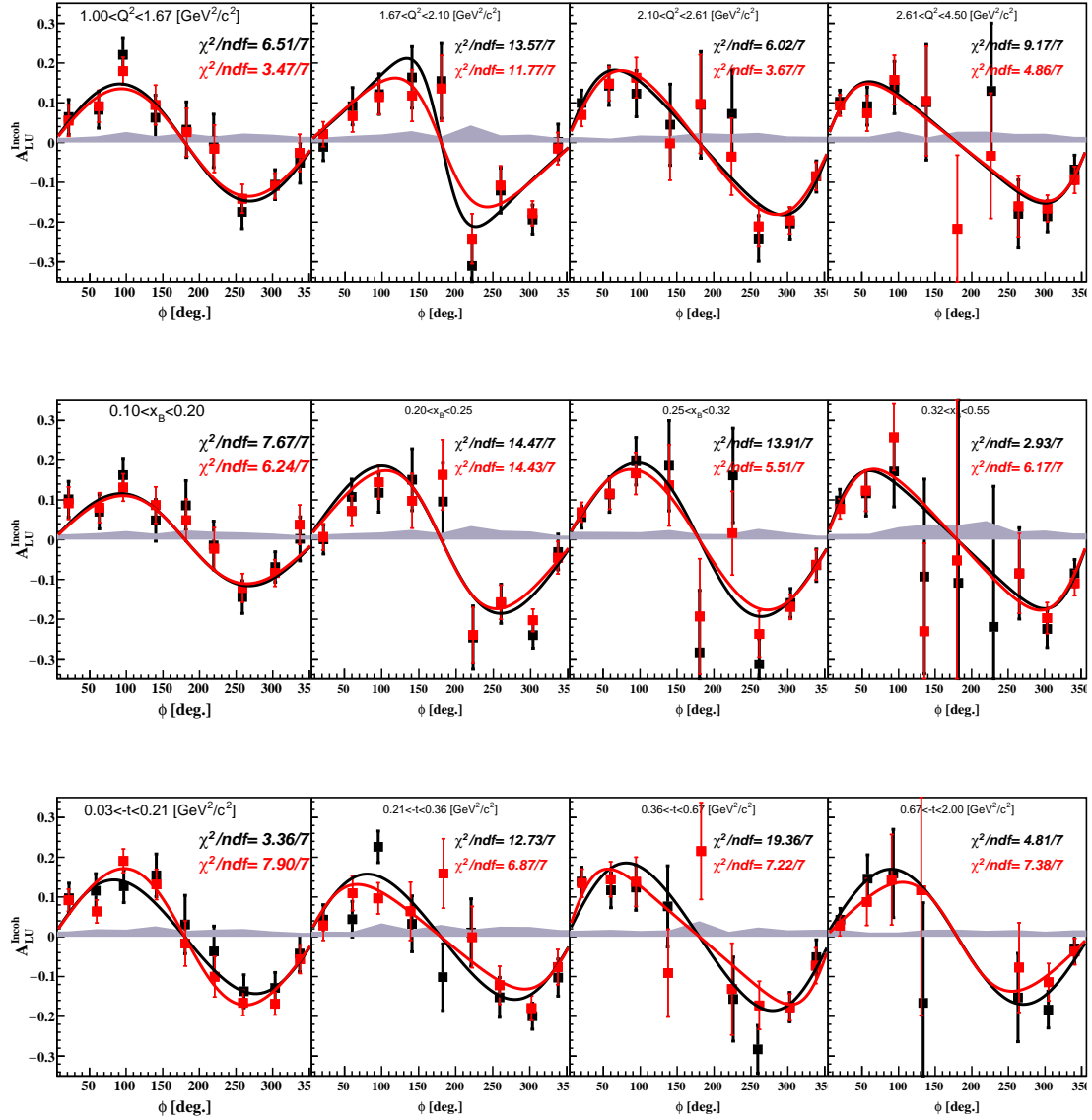


Figure 8: The EG6 incoherent  $A_{LU}$  as a function of  $\phi$ . Results are presented for different  $Q^2$  bins (top panel),  $x_B$  bins (middle panel), and  $t$  bins (bottom panel) using  $t$  in black points and using the corrected  $t'$  in red points. The red curves are the results of our fits with the form  $\frac{a \sin(\phi)}{1 + \beta \cos(\phi)}$ .

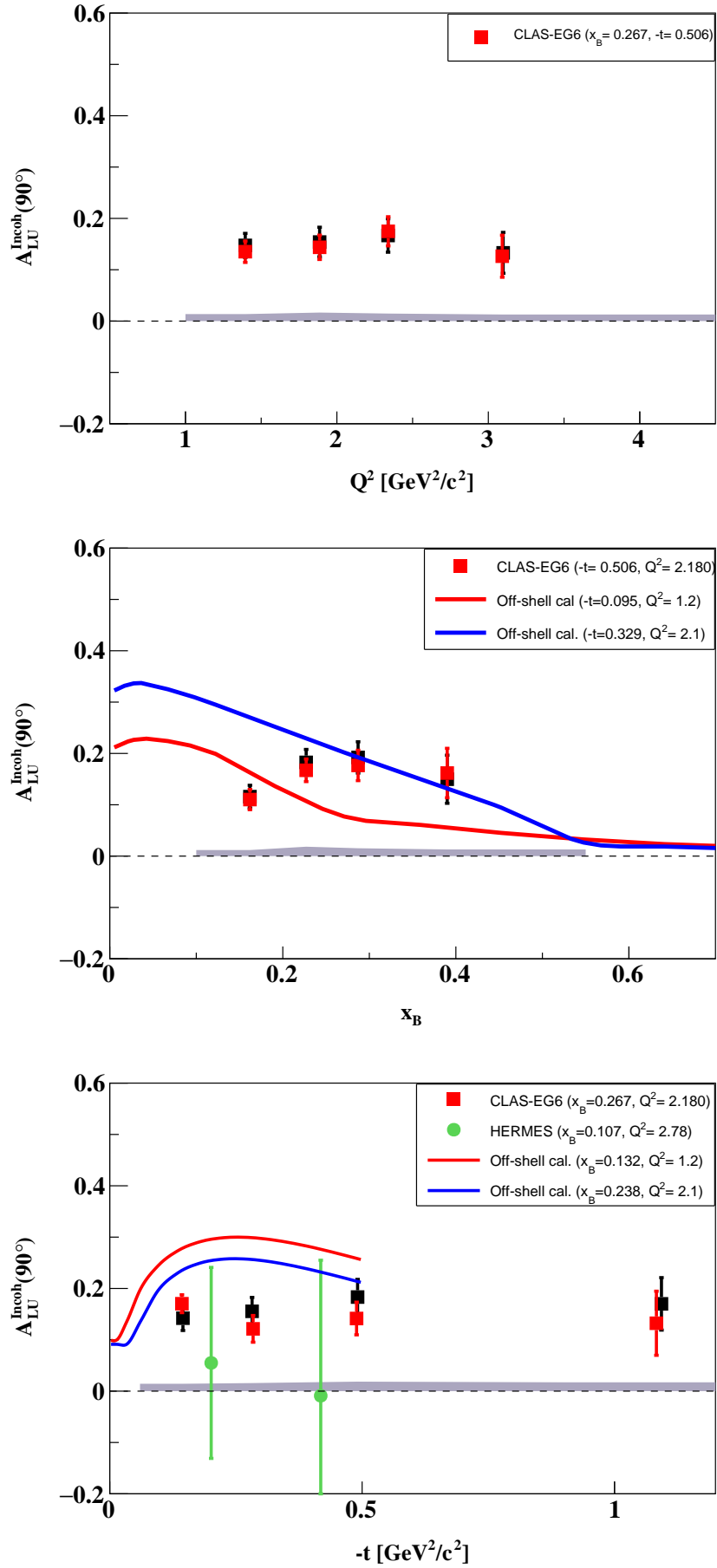


Figure 9: The EG6 incoherent  $Q^2$  (left),  $x_B$  (middle), and  $t$ -dependencies (right) of the  $A_{LU}$  at  $\phi = 90^\circ$  using  $t$  in black points and using the corrected  $t'$  in red points.